Radiotherapy and Oncology 138 (2019) 9–16

Contents lists available at ScienceDirect

Radiotherapy and Oncology

journal homepage: www.thegreenjournal.com

Original Article

A hepatocyte growth factor/MET-induced antiapoptotic pathway protects against radiation-induced salivary gland dysfunction

Yeo Jun Yoon, Hyun-Soo Shin, Jae-Yol Lim *

Department of Otorhinolaryngology, Yonsei University College of Medicine, Seoul, Republic of Korea

ARTICLE INFO

Article history:
Received 4 March 2019
Received in revised form 7 May 2019
Accepted 10 May 2019

Keywords:
Salivary gland
Radiation
Three-dimensional cell culture
Hepatocyte growth factor

ABSTRACT

Objective: Hepatocyte growth factor (HGF) and its receptor MET are expressed in the salivary glands during developmental stages and tumor formation; however, the function of HGF in injured salivary gland tissues remains unclear. The present study investigated the role of HGF in protecting the salivary glands against radiation-induced injury using an organotypic culture method.

Materials and methods: Acinar-like organoids were formed by means of a three-dimensional (3D) human parotid tissue-derived spheroids (hPTS) culture method. Radioprotective effects of HGF on irradiated hPTS and signaling pathways on radioprotection were investigated.

Results: We detected MET expression in hPTS grown in a 3D culture. Treatment of irradiated hPTS with recombinant human HGF (rhHGF) restored salivary marker expression and secretory function of hPTS. Changes in the phosphorylation levels of apoptosis-related proteins through HGF-MET axis inhibited radiation-induced apoptosis. Treatment with PHA665752, a MET inhibitor, blocked MET-PI3K-AKT pathway, increased apoptosis, and suppressed the radioprotective effect of rhHGF against IR-induced damage of hPTS.

Conclusions: These results suggest that HGF is a key effector of radioprotection and that HGF-MET-PI3K-AKT axis is involved in protecting the salivary glands from radiation-induced apoptosis.

Almost 500,000 patients are annually diagnosed with head and neck cancer worldwide, and many of them are treated with radiotherapy [1]. Despite recent advances in technology for decreasing radiation dose and volume reaching surrounding normal tissues, approximately 40% long-term cancer survivors develop irradiation (IR)-induced salivary gland hypofunction [2,3]. Salivary hypofunction leads to intractable xerostomia (dry mouth)-related complications such as oral soreness, mastication and swallowing difficulties, speech impairment, and increased oral infection and dental caries risk. Xerostomia significantly decreases the quality of life of patients, however, palliative management methods for xerostomia, such as the use of sialogogues or saliva substitutes, are only available in clinical setting. This highlights the need for developing radioprotection and/or regeneration strategies.

Cytoprotective agents, including biologic molecules, growth factors, and cytokines, have been suggested to protect or ameliorate radiation damage [4,5]. We used an organotypic three-dimensional (3D) human parotid tissue-derived spheroids (hPTS) culture method to show that IR-induced salivary hypofunction can be mitigated using growth factors that prevent human parotid epithelial cell (hPEC) apoptosis [6–8]. We recently found that adipose-derived mesenchymal stem cells (AdMSCs) under hypoxia inhibit the apoptosis of irradiated hPTS and hypoxia-stimulated AdMSCs secret several growth factors, including hepatocyte growth factor (HGF) [8,9]. Hepatocyte growth factor (HGF) is secreted during liver injury and promotes regeneration of damaged tissues [10]. HGF that is activated during tissue damage exerts antiapoptotic, proangiogenic, and mitogenic effects in various organs [11,12]. Xiong *et al.* suggested that HGF mRNA is highly expressed in the salivary glands of irradiated rats during recovery, implying that HGF plays a role in the cytoprotection of the salivary glands [13]. However, the exact role of HGF in the cytoprotection of the salivary glands is unclear.

The present study is the first to show that HGF exerts an antiapoptotic effect, prevents IR-induced apoptosis in salivary glands, and preserves the function of IR-damaged hPTS. Moreover, this study showed that HGF protects against IR-induced damage by activating MET-PI3K-AKT pathway. These results suggest that HGF is a key effector of radioprotection of the salivary glands.

Abbreviations: 3D, three-dimensional; HGF, hepatocyte growth factor; hPTS, human parotid tissue-derived spheroids; IR, irradiation.

* Corresponding author at: Department of Otorhinolaryngology, Gangnam Severance Hospital, Yonsei University College of Medicine, 211 Eonju-ro, Gangnam-gu, Seoul 06273, Republic of Korea.

E-mail address: jylimmd@yuhs.ac (J.-Y. Lim).

https://doi.org/10.1016/j.radonc.2019.05.012
0167-8140/

Materials and methods

Three-dimensional human parotid tissue-derived spheroid culture and in vitro irradiation

A specimen was obtained from a patient with benign tumor through parotidectomy after acquiring the patient's informed consent and approval from the institutional review board (IRB No. 2015-10-001). The obtained specimen was washed three times with 1× cold PBS (Gibco, Grand Island, NY, USA) containing 1% antibiotic, chopped, and incubated in HBSS (Gibco) containing 0.25% collagenase type II (2.5 mg/mL; Sigma-Aldrich, St. Louis, MO, USA) and DNase I (1 mg/mL; Sigma-Aldrich) with shaking at 37 °C for 30 min. Cell suspension obtained was filtered through a 70-μm cell strainer and centrifuged at 500×*g* for 5 min. Cell pellet obtained was cultured in a keratinocyte-serum-free medium (Gibco) supplemented with 5 ng/mL epidermal growth factor, 50 μg/mL bovine pituitary extract, 0.09 mM calcium chloride, and 1% antibiotic–antimycotic (Gibco). The cultured cells were seeded (density, 1×10^4 cells/cm^2) in a growth factor-reduced Matrigel (GFR-Matrigel)-precoated plate (Corning, Corning, NY, USA). The seeded hPECs were allowed to form three-dimensional (3D) spheroids on the GFR-Matrigel for 72 hours. Next, the cells were irradiated with 10-Gy radiation by using a 4-MV X-ray linear accelerator (Mevatron MD; Siemens Medical Laboratories Inc., Germany). The radiation dose was chosen based on IC50 dose used in our previous study [14].

Antibodies and reagents

Antibodies against MET (dilution, 1:1000), ZO-1 (dilution, 1:1000), phosphorylated PI3K (p-PI3K; Y508) (dilution, 1:1000), phosphorylated BCL-2 antagonist of cell death (BAD) (p-BAD; S136) (dilution, 1:1000), and β-actin (dilution, 1:1000) were obtained from Santa Cruz Biotechnology (Santa Cruz, CA, USA). Antibodies against α-amylase (α-Amy) (dilution, 1:1000), E-cadherin (dilution, 1:1000), phosphorylated p53 (p-p53; S15) (dilution, 1:1000), BAX (dilution, 1:1000), cleaved caspase-9 (dilution, 1:1000), cleaved caspase-3 (dilution, 1:1000), and BCL-2 (dilution, 1:1000) were obtained from Cell Signaling Technology (Danvers, MA, USA). Antibodies against phosphorylated γ-H2AX (S139) (dilution, 1:1000), phosphorylated AKT (p-AKT; S473) (dilution, 1:1000), phosphorylated MDM2 (p-MDM2; S166) (dilution, 1:1000), PTEN (dilution, 1:1000), and phosphorylated MET (p-MET; Y1230, Y1234, and Y1235) (dilution, 1:1000) were obtained from Abcam (England). Antibody against aquaporin 5 (AQP5) (dilution, 1:1000) was obtained from Calbiochem (San Diego, CA, USA). Recombinant human HGF (rhHGF) was purchased from R&D Systems, Minneapolis, MN, USA.

Western blotting analysis

Cell lysates were prepared using a whole cell lysis buffer containing 2% SDS (pH 6.8). Total proteins and histones present in the cell lysates were separated on an SDS–PAGE gel and were electrotransferred to a PVDF membrane. Proteins of interest were detected by incubating the membrane with the indicated primary antibodies. The experiment was repeated at least three times independently.

HGF concentration measurement

The concentration of hPEC-secreted HGF was measured by performing a sandwich enzyme-linked immunosorbent assay (ELISA) with a commercial kit (Quantikine; R&D Systems), according to the manufacturer's protocol. Samples from each group collected at different time points were assayed in triplicate, and absorbance was read at 450 nm. HGF concentration in each sample was determined by plotting optical density of the sample against a standard curve.

Cell viability assay

hPEC viability was determined by performing 3-(4,5-dimethyl thiazol-2-yl)-5-(3-carboxymethoxyphenyl)-2-(4-sulfophenyl)-2H-tetrazolium (MTS) assay. For this, 20 μL MTS (Promega Corporation, Madison, WI, USA) was added to each sample. After incubation for 1 hour, 100 μL mixture was transferred to a 96-well microplate and absorbance was measured at 490 nm. The experiment was repeated at least three times.

Terminal deoxynucleotidyl transferase dUTP nick end labeling assay

For performing terminal deoxynucleotidyl transferase dUTP nick end labeling (TUNEL) assay, hPTS were washed and fixed in 4% phosphate-buffered paraformaldehyde for 25 min at room temperature (RT). After washing three times with PBS, the cells were stained with *in Situ* Cell Death Detection Kit (Roche Diagnostics, Laval, Quebec, Canada), according to the manufacturer's protocol.

Immunofluorescence microscopy

For this, the hPTS were washed, fixed in 4% phosphate-buffered paraformaldehyde for 25 min at RT, and permeabilized with 0.4% Triton X-100 in 1× PBS for 10 min at RT. After washing three times with PBS, the spheroids were incubated for 1 hour in PBS containing 1% BSA, followed by overnight incubation at 4 °C with the primary antibodies against γ-H2AX, α-Amy, AQP5, E-cadherin, and ZO-1 that were diluted in PBS containing 1% BSA. After washing three times with PBS, the samples were incubated with primary antibody-specific secondary antibodies diluted in PBS for 1 hour at RT in a dark room and were washed three times with PBS. Nuclei were counterstained with DAPI. The samples were visualized under Axiovert 200 fluorescence microscope (Carl Zeiss, Goettingen, Germany) with 10 × 10 and 20 × 10NA objectives equipped with AxioCam HRC digital camera (Carl Zeiss).

Real-time polymerase chain reaction

Transcript levels were determined by performing real-time polymerase chain reaction (RT-PCR) with an ABI system and PowerUp™ SYBR™ Green Master Mix (Applied Biosystems, Foster City, CA, USA). PCR was performed in a 20 μL reaction mixture containing 50 ng cDNA, SYBR Green PCR master mix, and 10 pM sense and antisense primers specific for the genes encoding α-Amylase (*AMY1A*), Aquaporin 5 (*AQP5*), E-cadherin (*CDH1*), and ZO-1 (*TJP1*) (Table 1). Relative gene expression was quantified by normalizing with the housekeeping gene β-actin expression.

Table 1
Primers used for performing RT-PCR.

Gene and symbol		Primer sequences (5′-3′)
α-Amylase (*AMY1A*)	F	AATTGATCTGGGTGGTGAGC
	R	CTTATTTGGCGCCATCGATG
Aquaporin 5 (*AQP5*)	F	ACTGGGTTTTCTGGGTAGGG
	R	GTGGTCAGCTCCATGGTCTT
E-cadherin (*CDH1*)	F	CGCATTGCCACATACACTCT
	R	TTGGCTGAGGATGGTGTAAG
ZO-1 (*TJP1*)	F	TTTGGCCGAGGGATAGAAGT
	R	TATTGCCATCTCTTGCTGCC
Beta-actin (ACTB)	F	AGCTGTGCTATGTTGCCCTG
	R	AGGAAGCAAGGCTGGAAGAG

Amylase activity determination

Amylase activity in the secreted hPTS was determined using a salivary α-amylase assay kit (Salimetrics LLC, State College, PA, USA) with maltotriose-linked 2-chloro-p-nitrophenol as a chromogenic substrate, according to the manufacturer's instructions. Amylase activity in the sample was directly proportional to the increase in absorbance at 405 nm determined using a standard laboratory plate reader.

Statistical analysis

All experiments were performed at least three times. Results are presented as mean with standard deviation (SD). Statistical analyses were performed using GraphPad Prism 6.01 (GraphPad Software Inc., San Diego, CA, USA). $^{*}p < 0.05$, $^{**}p < 0.01$, $^{***}p < 0.001$, and $^{****}p < 0.0001$ were considered to be statistically significant, and $p > 0.05$ was considered statistically not significant.

Results

Human parotid epithelial cells express MET and rhHGF does not affect cell viability

First, we isolated and cultured human parotid epithelial cells (hPECs), as described previously [6]. MET expression was detected in both 2D hPEC and 3D hPTS cultures in Matrigel. However, RT-PCR and western blotting analysis showed that MET expression was higher in 3D hPTS culture than in 2D single-layered hPEC culture (Fig. 1A, B). Next, we measured the concentration of HGF secreted by hPECs in 2D culture by performing ELISA. HGF concentration was almost the same in cultures with and without hPECs, and there was no cumulative amount of hPECs up to 72-hour culture (Fig. 1C). Because HGF exerts a mitogenic effect, we examined whether HGF affected cell viability or growth in 2D culture under normal condition by performing trypan blue exclusion assay and MTS assay. Treatment with up to 200 ng/mL rhHGF did not affect cell viability or growth (Fig. 1D, E). Together, these results indicate that hPECs express MET, an HGF receptor, more in 3D spheroid culture but do not express HGF and that treatment with exogenous HGF under normal condition does not affect hPEC growth.

Exogenous rhHGF treatment prevents IR-induced DNA double-stranded breaks and apoptosis in a dose-dependent manner

We next investigated whether MET expression is activated after irradiation damage to salivary gland. hPTS was irradiated with 10-Gy, and the change in MET expression was confirmed by western blot. Expression of MET increased at 6 hours after irradiation, and eventually decreased over time (Fig. 2A). To explore the effects of exogenous rhHGF in inducing radioprotection against IR-induced damage in the salivary glands, hPTS were then incubated with 50, 100, and 200 ng/mL rhHGF immediately after IR. Treatment with rhHGF significantly improved the cell viability and morphology of hPTS in a dose-dependent manner at 48 hours after treatment with 10-Gy radiation compared with those of irradiated cells not treated with rhHGF (Fig. 2B, C). Assessment of the effect of rhHGF on the recovery of cell viability and morphology suggested that 100 ng/mL was effective concentration of rhHGF. Therefore, this rhHGF concentration was used for performing subsequent experiments.

Next, we investigated whether IR induced apoptosis by performing TUNEL assay, which detects apoptotic DNA fragments or extreme DNA damage [17]. The number of TUNEL-positive cells significantly decreased after rhHGF treatment (Fig. 3A). Moreover,

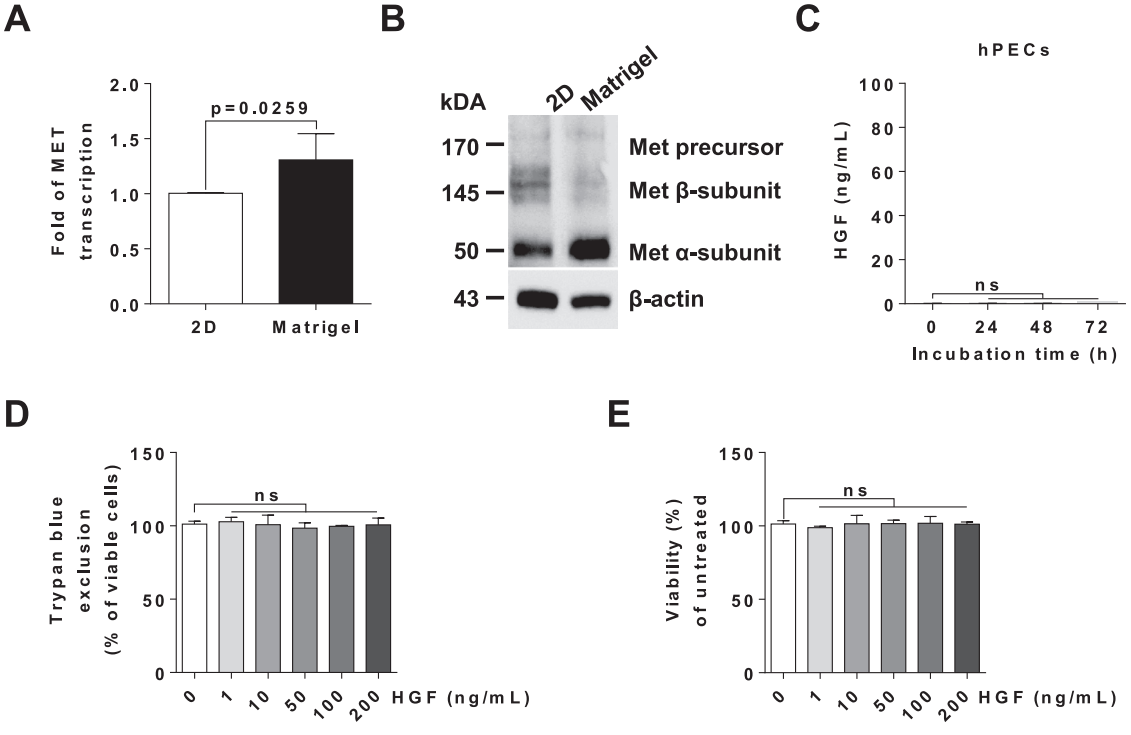

Fig. 1. Characterization of hPECs. (A) MET mRNA level in the 2D hPEC and 3D hPTS cultures. Relative fold change in the mRNA expression level of each gene was normalized using the mRNA expression level of the β-actin gene ($n = 6$ for each group); p values were determined using an unpaired t-test with Welch's correction. (B) Expression levels of MET precursor and subunits in the 2D and 3D cultures. (C) Determination of the concentration of HGF secreted by hPECs in culture medium. (D and E) Relative cell viability was determined by performing the trypan blue exclusion and MTS assays. Results are expressed as mean ± SD ($n = 3$); p values shown in (D and E) were determined using one-way analysis of variance (ANOVA) with Bonferroni's post-hoc test.

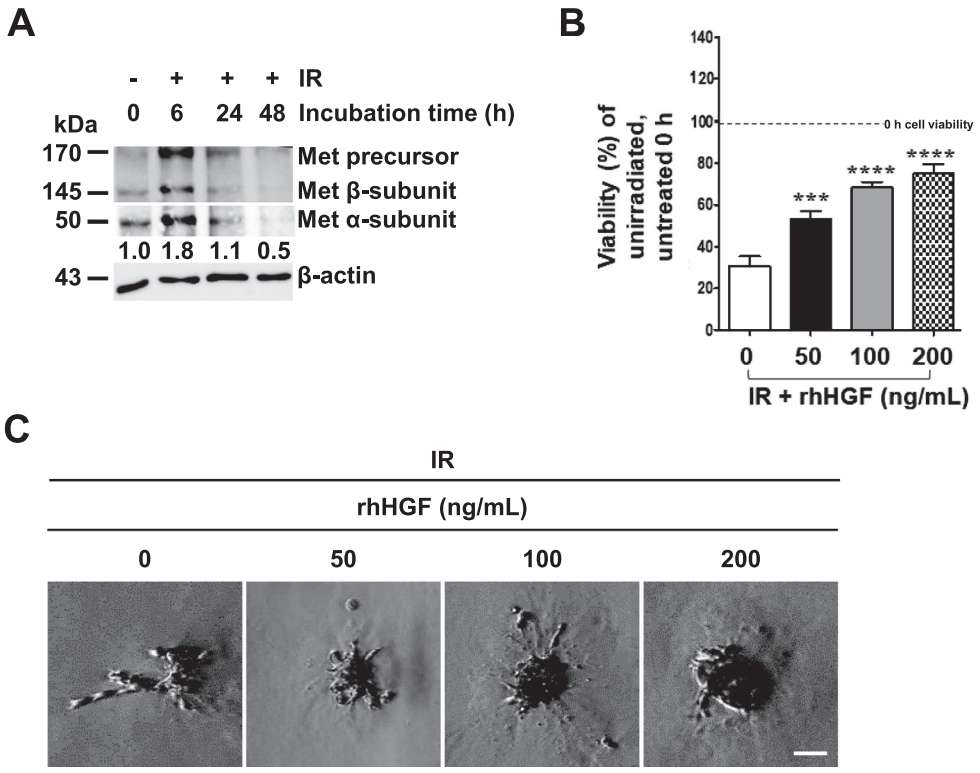

Fig. 2. HGF treatment inhibits the apoptosis of irradiated hPTS. (A) Expression levels of MET in the hPTS irradiated with 10-Gy radiation and incubated for 48 hours were determined by performing western blotting analysis, with β-actin as the loading control. (B and C) Treatment of hPTS with the indicated concentration of HGF immediately after IR. (B) Relative cell viability was measured by performing the MTS assay at 48 hours after the IR. Results are expressed as mean ± SD (n = 3); p values were determined using ANOVA with the Bonferroni's post-hoc test. (C) Difference in the morphology of the irradiated hPTS; scale bars represent 20 μm.

the number of TUNEL-positive cells was higher in irradiated hPTS than non-irradiated hPTS. Next, we assessed DNA double-stranded breaks (DNA-DSBs) and apoptotic DNA fragmentation by performing γ-H2AX immunofluorescence staining. We observed that rhHGF treatment decreased the proportion of DNA-DSBs (Fig. 3B). To elucidate mechanisms underlying IR-induced apoptosis, we explored changes in the expression of apoptosis-related proteins. Expression levels of p-p53, its proapoptotic target BAX, cleaved caspase-9, and cleaved caspase-3 increased and that of the antiapoptotic protein BCL-2 decreased after IR (Fig. 3C, lane 2). However, treatment of rhHGF decreased IR-induced apoptosis and proapoptotic protein expression in hPTS (Fig. 3C, lane 3). Densitometric analysis of the results of western blotting analysis clearly showed the changes in the apoptosis-related protein levels (Fig. 3D). Together, these data suggest that rhHGF exerts antiapoptotic effects on IR-damaged hPTS by inhibiting an apoptosis pathway.

Exogenous rhHGF treatment protects and rescues the function of hPTS from IR-induced damage

We previously found that irradiated hPTS cultured in GFR-Matrigel showed the loss of structural protein expression and secretory function [6]. Therefore, we investigated whether exogenous rhHGF treatment maintained the structure and function of irradiated hPTS. Fluorescence microscopy indicated that the expression of acinar markers α-Amy and AQP5 markedly decreased (Fig. 4A, row 2) and that the expression of epithelial cell markers E-cadherin and ZO-1 was negligible in irradiated hPTS. However, rhHGF treatment immediately after the IR increased the expression of the acinar and epithelial cell markers in hPTS (Fig. 4A, row 3). Western blotting analysis also showed that the expression of the acinar and epithelial cell markers decreased in the lysates of irradiated hPTS (Fig. 4B, lane 2) compared with that in the lysates of non-irradiated hPTS (Fig. 4B, lane 1) and increased in the lysates of irradiated hPTS treated with rhHGF (Fig. 4B lane 3). Consistently, RT-PCR showed that rhHGF treatment rescued the expression of the salivary acinar and epithelial cell marker genes (Fig. 4C). hPTS secrete amylase [18]. Next, we measured amylase activity to confirm that rhHGF treatment restored the secretory function of irradiated hPTS. Treatment of irradiated hPTS with rhHGF significantly increased the amylase activity (Fig. 4D). Together, these results indicate that rhHGF treatment recovers structural protein expression in and secretory function of irradiated hPTS.

Recombinant human HGF treatment induces radioprotection by exerting an antiapoptotic effect by activating the MET-PI3K-AKT pathway

Next, we explored whether the binding of HGF to its receptor HGFR/MET activated PI3K-AKT signaling pathway as a radioprotective mechanism. PI3K-AKT pathway promotes cell survival by inactivating proapoptotic effectors such as BAD and by suppressing p53-mediated apoptotic signaling through the activation of MDM2, a p53-interacting protein that downregulates p53 transcriptional activity [19,20]. In the present study, IR decreased the phosphorylation of MET, PI3K, AKT, BAD, and MDM2 and increased the expression of PTEN in hPTS (Fig. 5A, lane 2). However, rhHGF treatment increased the phosphorylation of MET, PI3K, AKT, BAD, and MDM2 and decreased the expression of PTEN (Fig. 5A, lane 3). Blockade of the binding of HGF to MET by using an MET inhibitor PHA665752 decreased the phosphorylation of MET, PI3K, AKT, and MDM2 (Fig. 5A, lane 4). Results of the cell viability assay showed that PHA665752 treatment decreased the viability of the

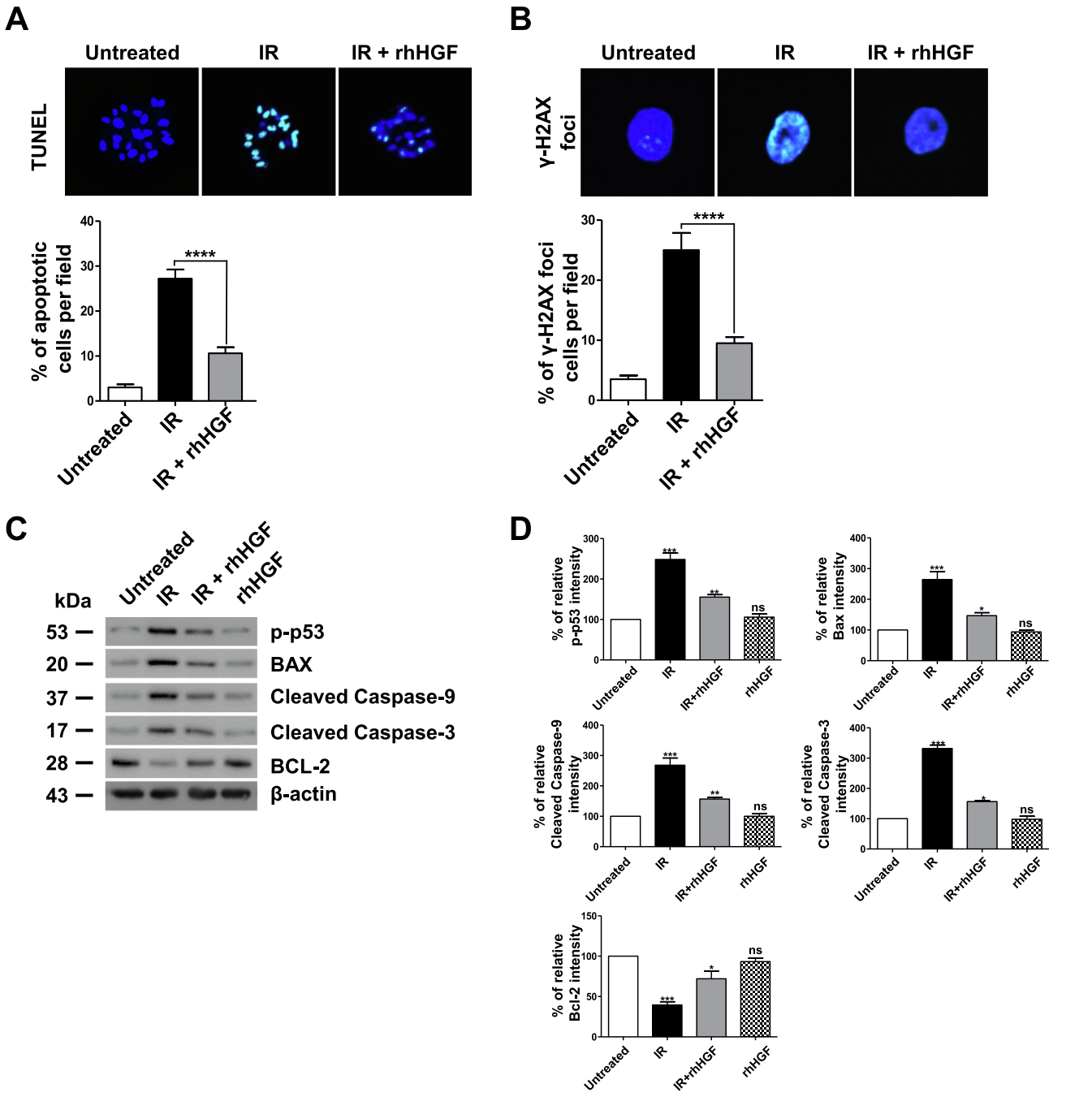

Fig. 3. HGF treatment inhibits the intrinsic apoptosis pathway in irradiated hPTS. (A and B) Representative images of the TUNEL assay and γ-H2AX immunofluorescence microscopy of hPTS treated with 10-Gy IR and incubated for up to 48 hours. Nuclei were counterstained with DAPI. Representative results are shown in the upper panels, and average number of TUNEL-positive cells and γ-H2AX foci in the irradiated hPTS compared with those in non-irradiated hPTS are shown in the lower panels. Results are expressed as mean ± SD (n = 3); p values shown in (A and B) were determined using ANOVA with the Bonferroni's post-hoc test. (C) Expression levels of p-p53, BAX, cleaved caspase-9, cleaved caspase-3, and BCL-2 in the hPTS irradiated with 10-Gy radiation and incubated for 48 hours were determined by performing western blotting analysis, with β-actin as the loading control. (D) Densitometric analysis of IR-induced alterations in apoptosis-related protein levels. Data were normalized using β-actin protein level. Normalization intensity was analyzed and presented as mean ± SD (n = 3); p values were determined using ANOVA with the Bonferroni's post-hoc test.

irradiated hPTS in the presence of rhHGF (Fig. 5B), which was consistent with the results presented in Fig. 5A. However, rhHGF treatment significantly improved the morphology and structural protein expression in hPTS compared with those in rhHGF-untreated irradiated hPTS and PHA665752-treated hPTS (Fig. 5C, D). These results suggest that rhHGF induces radioprotection by exerting an antiapoptotic effect by activating MET-PI3K-AKT pathway.

Discussion

Radiation-induced salivary gland dysfunction is attributed to the destruction of terminally differentiated salivary gland cells and/or loss of regenerative capacity of tissue-resident stem cells or progenitor cells [21]. Preservation or restoration of salivary gland function can be achieved by protecting salivary gland cells from IR. We recently established an organotypic hPTS mimicking

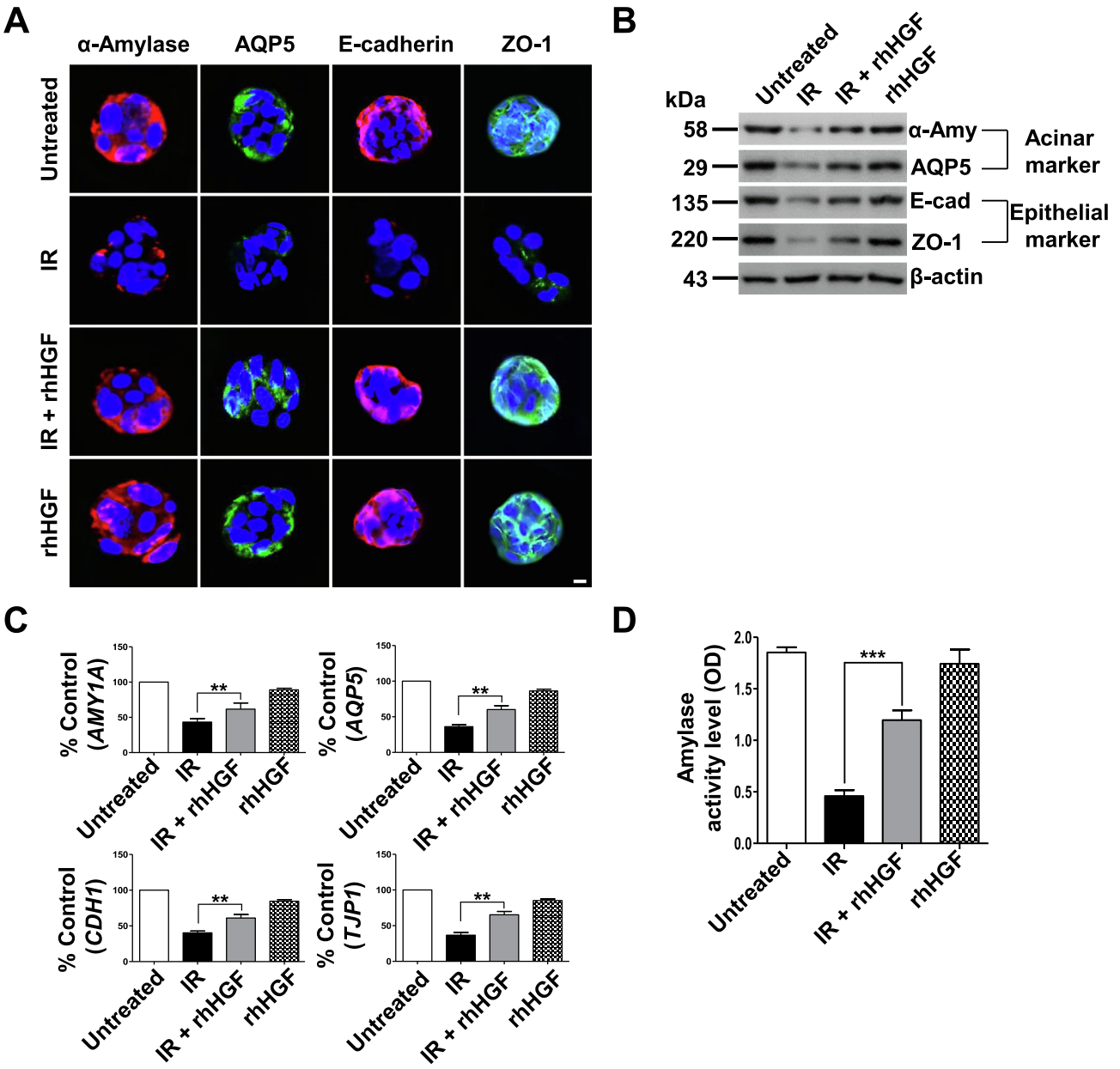

Fig. 4. Effects of HGF on the structure and function of irradiated hPTS in 3D culture. (A) Immunofluorescence images showing the expression of acinar markers α-Amy (red) and AQP5 (green), epithelial protein E-cadherin (red), and tight junction (TJ)-associated protein ZO-1 (green). Nuclei were stained with DAPI (blue). Scale bars represent 10 μm. (B) Protein expression of the salivary acinar markers (α-Amy and AQP5), adherent protein (E-cadherin), and TJ-associated protein (ZO-1) was determined by performing western blotting analysis, with β-actin as the loading control. (C) The mRNA expression of the genes encoding these proteins was determined by performing RT-PCR. Results are expressed as mean ± SD ($n = 3$). (D) Amylase secretion from the hPTS was determined using an assay kit. Results are expressed as mean ± SD ($n = 3$); p values shown in (C and D) were determined using ANOVA with the Bonferroni's post-hoc test. (For interpretation of the references to colour in this figure legend, the reader is referred to the web version of this article.)

irradiation-induced salivary hypofunction, by which we could evaluate the efficacy of a key factors released from stem cells by paracrine effect without direct cell-to-cell contact or animal experiments [6,14]. We employed organotypic hPTS culture in this study and found that radiotoxic cell death of irradiated hPTS can be alleviated by administration of rhHGF. We observed that exogenous rhHGF treatment inhibited the apoptosis in irradiated hPTS. The rhHGF-treated cells showed deceased DNA fragmentation or DNA-DSBs after IR, as determined by performing the TUNEL assay or γ-H2AX immunofluorescence staining. The rhHGF decreased proapoptotic protein levels and increased antiapoptotic protein levels. Furthermore, rhHGF treatment restored epithelial cell marker expression and α-amylase activity in hPTS in 3D culture. These results suggest that HGF functions as a key effector of radioprotection against IR-induced salivary gland dysfunction by interacting with MET.

HGF/MET signaling involves various essential biologic activities in cells during development, regeneration, as well as progression to solid tumors [11]. Although the physiologic function of HGF by binding to MET in salivary glands has been reported during branching morphogenesis [22,23], the exact role of HGF remains undetermined in adult salivary glands. In developing salivary glands, HGF and MET expressions have been noted in ductal cells and stroma during developmental process [24]. However, MET expression has not been observed neither in the membrane of adult salivary ductal cells nor in acinar cells, whereas MET was

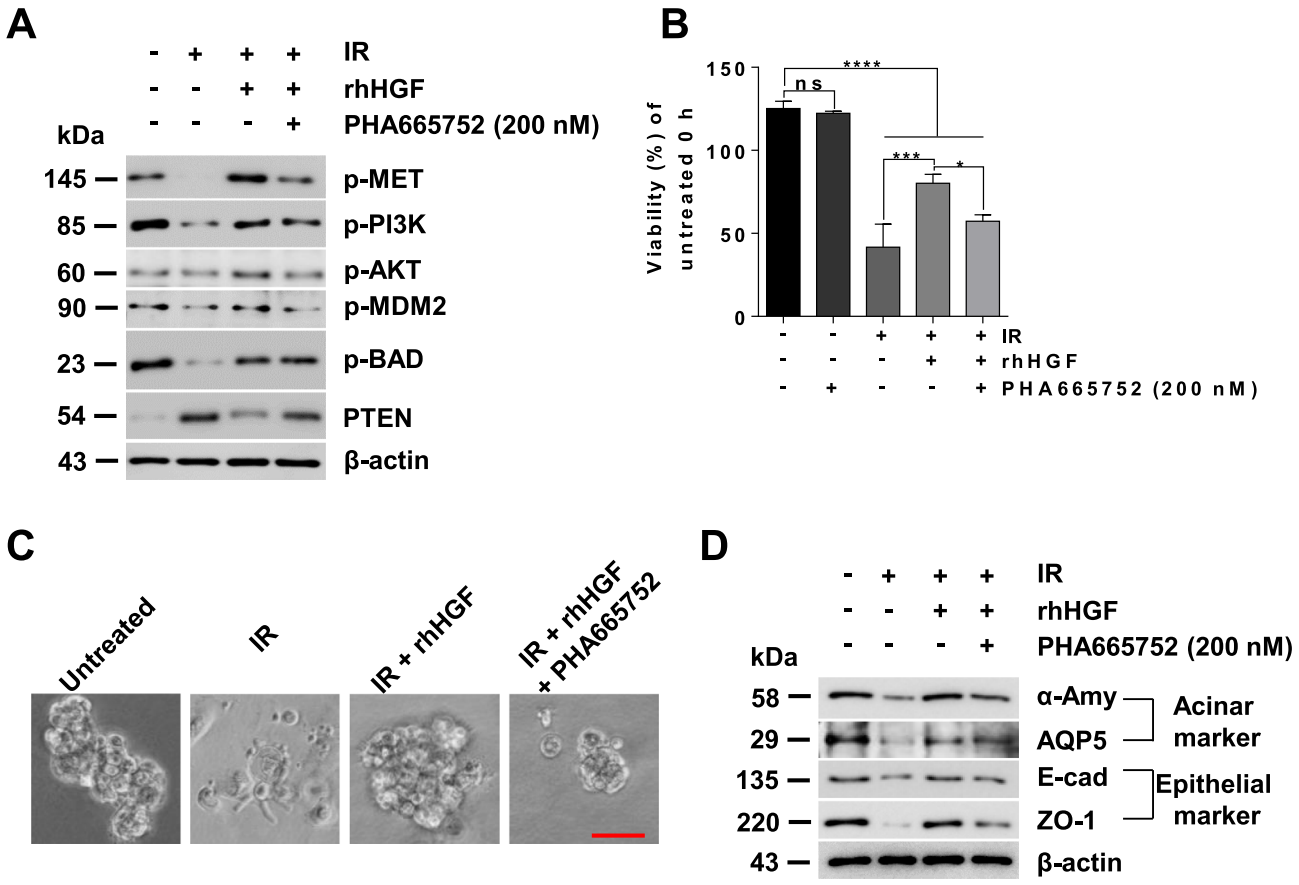

Fig. 5. Mechanism underlying the antiapoptotic effect of HGF through the MET-PI3K-AKT axis. (A–D) Supplementation of the hPEC culture medium with the indicated concentration of HGF immediately after IR. (A) Expression levels of p-MET, p-PI3K, p-AKT, p-BAD, p-MDM2, and PTEN were determined by performing western blotting analysis, with β-actin as the loading control. (B) Relative cell viability was measured by performing the MTS assay. Results are expressed as mean ± SD ($n = 3$); p values were determined using ANOVA with the Bonferroni's post-hoc test. (C) Difference in the morphology of the irradiated hPTS; scale bars represent 50 μm. (D) Protein levels of the salivary acinar markers (α-Amy and AQP5), adherent protein (E-cadherin), and TJ-associated protein (ZO-1) were determined by performing western blotting analysis, with β-actin as the loading control.

usually expressed in acinar or ductal cell membranes of other glandular organs, including the pancreas and liver [15,16]. Some studies have reported that increased HGF and MET expression levels after radiation injury, which indicates regeneration potential of HGF in salivary glands [25–27]. These highlight the importance of assessing reparative or regenerative roles of HGF/MET pathway in salivary glands. In this study, we showed MET expression in 3D hPTS and 2D hPEC cultures. Treatment with rhHGF exerted the antiapoptotic effect through MET-PI3K-AKT pathway, and these effects of rhHGF were abrogated after treatment with MET inhibitor PHA665752. These results imply that HGF/MET interaction involves radioprotection against IR-induced salivary gland dysfunction [28,29]. Meanwhile, HGF/MET expressions were also observed in ductal cells of benign or malignant salivary neoplasms [24,30].

A recent study also showed that the inhibition of HGF/MET pathway increases susceptibility to radiation therapy [31], which is consistent with the results obtained using MET inhibitor in the present study. Given that MET expression was also observed in benign or malignant salivary neoplasms, more attention is needed to harness HGF/MET pathway as a protective mechanism in salivary gland cancer patients.

In this study, we adapted 10-Gy radiation dose as the radiation dose at the level of IC50 referred from our previous study, and used experimental conditions that have been described elsewhere [14,32]. However, radiotherapy involves the use of a cumulative dose of 50–70 Gy (e.g. 2 Gy/day). Therefore, animal experiments are required to determine the appropriate dosage and administration frequency of rhHGF for application in human patients. It should be also noted that this hPTS culture model may not represent various responses to radiation damage, since radiation responses are complex *in vivo* according to interaction between cells and their microenvironment as well as even between individuals *in vivo*. Nevertheless, this IR experiment using 3D spheroid culture enables elucidation of IR-induced cellular death mechanism, providing information vital to the development of preventive and therapeutic candidates against IR damage because IR to hPTS assembled as acinar-like 3D structures were shown to be capable of representing IR-induced SG hypofunction *in vivo* [14].

HGF exerts other cytoprotective effects such as inhibition of autophagic cell death [33] and regulation of inflammation [34,35]. Moreover, the body removes damaged cells and initiates regeneration by inducing cell death and inflammation [36]. Therefore, additional studies are needed to assess whether exogenous HGF treatment affects these processes, which may affect the expected outcomes of this treatment. Lastly, salivary paracrine factors such as epidermal growth factor (EGF), fibroblast growth factor (FGF), and insulin-like growth factor 1 (IGF-1) can also protect irradiation-damaged salivary cells in a synergistic way [31,37,38]. Therefore, the complexity of action mechanisms of growth factors involving tissue repair and/or regeneration in salivary glands remains to be determined.

In conclusion, we examined the expression of MET and the role of exogenous rhHGF in preserving the structure and secretory

function of irradiated hPTS in a 3D culture. Treatment with rhHGF suppressed the IR-induced apoptosis in irradiated hPTS and preserved the structural marker expression and secretory function of hPTS. Treatment with MET inhibitor blocked MET-PI3K-AKT pathway, increased apoptosis, and suppressed the radioprotective effect of rhHGF against IR-induced structural alteration and dysfunction, suggesting that HGF acts as a key effector of radioprotection by modulating MET-PI3K-AKT pathway. Although additional studies are needed, the present study is the first to suggest the potential of HGF for protecting the salivary glands from IR-induced damage, and its results indicated that hPTS culture as a reliable new *ex vivo* model for screening radioprotective agents.

Declaration of Competing Interest

The authors declare that they do not have any potential conflicts of interest related to this study.

Acknowledgements

This work is supported by the Stem Cell Research Project through the National Research Foundation of Korea (NRF) funded by the Ministry of Education, Science and Technology (NRF-2017M3A9B4032053) and by the Basic Science Research Program through the NRF funded by the Ministry of Science and ICT (NRF-2018R1A2B3004269), Republic of Korea.

References

[1] Jemal A, Bray F, Center MM, Ferlay J, Ward E, Forman D. Global cancer statistics. CA Cancer J Clin 2011;61:69–90.
[2] Haddad RI, Shin DM. Recent advances in head and neck cancer. N Engl J Med 2008;359:1143–54.
[3] Galvao-Moreira LV, Santana T, da Cruz MC. A closer look at strategies for preserving salivary gland function after radiotherapy in the head and neck region. Oral Oncol 2016;60:137–41.
[4] van Luijk P, Pringle S, Deasy JO, Moiseenko VV, Faber H, Hovan A, et al. Sparing the region of the salivary gland containing stem cells preserves saliva production after radiotherapy for head and neck cancer. Sci Transl Med 2015;7:305ra147.
[5] Bhide SA, Miah AB, Harrington KJ, Newbold KL, Nutting CM. Radiation-induced xerostomia: pathophysiology, prevention and treatment. Clin Oncol-Uk 2009;21:737–44.
[6] Shin HS, Lee S, Kim YM, Lim JY. Hypoxia-activated adipose mesenchymal stem cells prevents irradiation-induced salivary hypofunction by enhanced paracrine effect through fibroblast growth factor 10. Stem Cells 2018;36:1020–32.
[7] Choi JS, Shin HS, An HY, Kim YM, Lim JY. Radioprotective effects of Keratinocyte Growth Factor-1 against irradiation-induced salivary gland hypofunction. Oncotarget 2017;8:13496–508.
[8] An HY, Shin HS, Choi JS, Kim HJ, Lim JY, Kim YM. Adipose mesenchymal stem cell secretome modulated in hypoxia for remodeling of radiation-induced salivary gland damage. PLoS ONE 2015;10:e0141862.
[9] Weil BR, Markel TA, Herrmann JL, Abarbanell AM, Meldrum DR. Mesenchymal stem cells enhance the viability and proliferation of human fetal intestinal epithelial cells following hypoxic injury via paracrine mechanisms. Surgery 2009;146:190–7.
[10] Nakamura T, Nawa K, Ichihara A. Partial-purification and characterization of hepatocyte growth-factor from serum of hepatectomized rats. Biochem Biophy Res Co 1984;122:1450–9.
[11] Nakamura T, Sakai K, Nakamura T, Matsumoto K. Hepatocyte growth factor twenty years on: Much more than a growth factor. J Gastroenterol Hepatol 2011;26(Suppl 1):188–202.
[12] Vogel S, Borger V, Peters C, Forster M, Liebfried P, Metzger K, et al. Necrotic cell-derived high mobility group box 1 attracts antigen-presenting cells but inhibits hepatocyte growth factor-mediated tropism of mesenchymal stem cells for apoptotic cell death. Cell Death Differ 2015;22:1219–30.
[13] Xiong XY, Shi XJ, Chen FS. Human adipose tissue-derived stem cells alleviate radiation-induced xerostomia. Int J Mol Med 2014;34:749–55.
[14] Shin HS, An HY, Choi JS, Kim HJ, Lim JY. Organotypic spheroid culture to mimic radiation-induced salivary hypofunction. J Dent Res 2017;96:396–405.
[15] Alvarez-Perez JC, Ernst S, Demirci C, Casinelli GP, Mellado-Gil JMD, Rausell-Palamos F, et al. Hepatocyte growth factor/c-met signaling is required for beta-cell regeneration. Diabetes 2014;63:216–23.
[16] Ishikawa T, Factor VM, Marquardt JU, Raggi C, Seo D, Kitade M, et al. Hepatocyte growth factor/c-met signaling is required for stem-cell-mediated liver regeneration in mice. Hepatology 2012;55:1215–26.
[17] Lozano GM, Bejarano I, Espino J, Gonzalez D, Ortiz A, Garcia JF, et al. Relationship between caspase activity and apoptotic markers in human sperm in response to hydrogen peroxide and progesterone. J Reprod Develop 2009;55:615–21.
[18] Chan YH, Huang TW, Young TH, Lou PJ. Human salivary gland acinar cells spontaneously form three-dimensional structures and change the protein expression patterns. J Cell Physiol 2011;226:3076–85.
[19] Xu R, Sun Y, Chen Z, Yao Y, Ma G. Hypoxic preconditioning inhibits hypoxia-induced apoptosis of cardiac progenitor cells via the PI3K/Akt-DNMT1-p53 pathway. Sci Rep 2016;6:30922.
[20] Qiu W, Leibowitz B, Zhang L, Yu J. Growth factors protect intestinal stem cells from radiation-induced apoptosis by suppressing PUMA through the PI3K/AKT/p53 axis. Oncogene 2010;29:1622–32.
[21] Pringle S, Van Os R, Coppes RP. Concise review: adult salivary gland stem cells and a potential therapy for xerostomia. Stem Cells 2013;31:613–9.
[22] Ikari T, Hiraki A, Seki K, Sugiura T, Matsumoto K, Shirasuna K. Involvement of hepatocyte growth factor in branching morphogenesis of murine salivary gland. Dev Dyn 2003;228:173–84.
[23] Loreto C, Caltabiano R, Musumeci G, Caltabiano C, Greco MG, Leonardi R. Hepatocyte growth factor receptor, c-Met, in human embryo salivary glands. An immunohistochemical study. Anatomia, Histologia, Embryologia 2010;39:173–7.
[24] Tsukinoki K, Yasuda M, Asano S, Karakida K, Ota Y, Osamura RY, et al. Association of hepatocyte growth factor expression with salivary gland tumor differentiation. Pathol Int 2003;53:815–22.
[25] Chi CH, Liu IL, Lo WY, Liaw BS, Wang YS, Chi KH. Hepatocyte growth factor gene therapy prevents radiation-induced liver damage. World J Gastroentero 2005;11:1496–502.
[26] Qian LW, Mizumoto K, Inadome N, Nagai E, Sato N, Matsumoto K, et al. Radiation stimulates HGF receptor/c-Met expression that leads to amplifying cellular response to HGF stimulation via upregulated receptor tyrosine phosphorylation and map kinase activity in pancreatic cancer cells. Int J Cancer 2003;104:542–9.
[27] Soh HE, Bhardwaj V, Cortez MA, Allen PK, Heymach JV, Meyn R, et al. HGF is associated with radioresistance and local recurrence in non-small cell lung cancer. Int J Radiat Oncol 2013;87:S652-S.
[28] Bhardwaj V, Cascone T, Cortez MA, Amini A, Evans J, Komaki RU, et al. Modulation of c-met signaling and cellular sensitivity to radiation potential implications for therapy. Cancer-Am Cancer Soc 2013;119:1768–75.
[29] Hu SY, Duan HF, Li QF, Yang YF, Chen JL, Wang LS, et al. Hepatocyte growth factor protects endothelial cells against gamma ray irradiation-induced damage. Acta Pharmacol Sin 2009;30:1415–20.
[30] Accornero P, Miretti S, Bersani F, Quaglino E, Martignani E, Baratta M. Met receptor acts uniquely for survival and morphogenesis of EGFR-dependent normal mammary epithelial and cancer cells. PLoS ONE 2012;7:e44982.
[31] Limesand KH, Barzen KA, Quissell DO, Anderson SM. Synergistic suppression of apoptosis in salivary acinar cells by IGF1 and EGF. Cell Death Differ 2003;10:345–55.
[32] Smirnov DA, Morley M, Shin E, Spielman RS, Cheung VG. Genetic analysis of radiation-induced changes in human gene expression. Nature 2009;459:587–91.
[33] Gallo S, Gatti S, Sala V, Albano R, Costelli P, Casanova E, et al. Agonist antibodies activating the Met receptor protect cardiomyoblasts from cobalt chloride-induced apoptosis and autophagy. Cell Death Dis 2014;5.
[34] Wang H, Sun RT, Li Y, Yang YF, Xiao FJ, Zhang YK, et al. Gene modification in mesenchymal stem cells reduces radiation-induced intestinal injury by modulating immunity. PLoS ONE 2015;10.
[35] Coudriet GM, He J, Trucco M, Mars WM, Piganelli JD. Hepatocyte growth factor modulates interleukin-6 production in bone marrow derived macrophages: implications for inflammatory mediated diseases. PLoS ONE 2010;5.
[36] Poon IKH, Lucas CD, Rossi AG, Ravichandran KS. Apoptotic cell clearance: basic biology and therapeutic potential. Nat Rev Immunol 2014;14:166–80.
[37] Thula TT, Schultz G, Tran-Son-Tay R, Batich C. Effects of EGF and bFGF on irradiated parotid glands. Ann Biomed Eng 2005;33:685–95.
[38] Martin KL, Hill GA, Klein RR, Arnett DG, Burd R, Limesand KH. Prevention of radiation-induced salivary gland dysfunction utilizing a CDK inhibitor in a mouse model. PLoS ONE 2012;7:e51363.